

# Adaptive Latent Space Tuning for Non-Stationary Distributions

**Alexander Scheinker\***

Accelerator Operations and Technology  
Los Alamos National Laboratory

**Frederick Cropp**

Department of Physics and Astronomy  
University of California Los Angeles

**Sergio Paiagua**

Advanced Light Source Accelerator Physics  
Lawrence Berkeley National Laboratory

**Daniele Filippetto**

Advanced Light Source Accelerator Physics  
Lawrence Berkeley National Laboratory

## Abstract

Powerful deep learning tools, such as convolutional neural networks (CNN), are able to learn the input-output relationships of large complicated systems directly from data. Encoder-decoder deep CNNs are able to extract features directly from images, mix them with scalar inputs within a general low-dimensional latent space, and then generate new complex 2D outputs which represent complex physical phenomenon. One important challenge faced by deep learning methods is large non-stationary systems whose characteristics change quickly with time for which re-training is not feasible. In this paper we present a method for adaptive tuning of the low-dimensional latent space of deep encoder-decoder style CNNs based on real-time feedback to quickly compensate for unknown and fast distribution shifts. We demonstrate our approach for predicting the properties of a time-varying charged particle beam in a particle accelerator whose components (accelerating electric fields and focusing magnetic fields) are also quickly changing with time.

## 1 Introduction

Powerful machine learning (ML)-based tools are now being used in almost all fields of scientific research [1–4]. The growth of ML is due to a combination of the development of advanced algorithms such as convolutional neural networks (CNN) [5], spatial transformer networks [6–8], recurrent neural networks [9, 10], analytical studies which have improved the understanding of deep learning characteristics [11, 12], deep reinforcement learning [13, 14], the availability of affordable high performance computing (graphics processing units), and powerful open source ML packages such as TensorFlow [15, 16], Caffe [17], CNTK [18], Theano [19], and PyTorch [20].

### 1.1 ML Applications

Examples of ML applications for physical systems include molecular and materials science studies [21], for use in optical communications and photonics [22], for studying glassy systems [23–25], to accurately predict battery life in [26], to accelerate lattice Monte Carlo simulations using neural networks [27], for studying complex networks [28], for characterizing surface microstructure of complex materials [29], for chemical discovery [30], for active matter analysis by using deep neural networks to track objects [31], for particle physics [32], for antimicrobial studies [33], for pattern recognition for optical microscopy images of metallurgical micro-structures [34], for learning Perovskit bandgaps [35], for real-time mapping of electron backscatter diffraction (EBSD) patterns

\*Correspondence: [ascheink@lanl.gov](mailto:ascheink@lanl.gov).

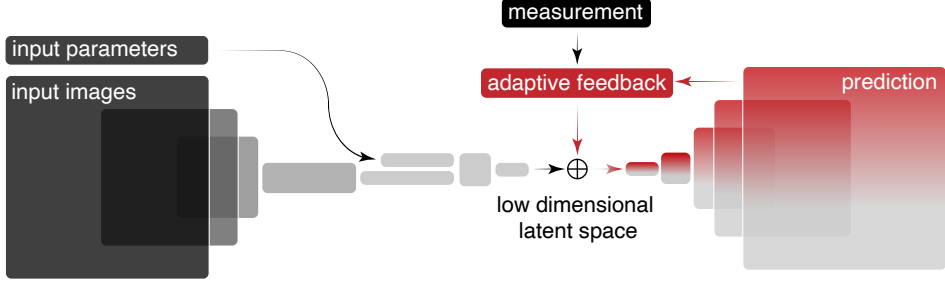


Figure 1: Adaptive machine learning setup for an encoder-decoder style 2D convolutional neural network with additional scalar parameter inputs. For example, the size of an input image is first reduced using 2D convolution layers with stride lengths greater than 1 before being flattened and concatenated with an input vector of parameters, both of which are then passed through fully connected dense layers and transformed into a low dimensional latent space. For example, below we use 5 input parameters and  $52 \times 52$  pixel single channel input images for a total input dimension of 2709, which is then squeezed down to a 100 dimensional latent space vector to which we add a 100 dimensional adaptively tuned input vector based on feedback.

to crystal orientations [36], for speeding up simulation-based accelerator optimization studies [37], for Bayesian optimization of free electron lasers (FEL) [38], for temporal power reconstruction of FELs [39], for various applications at the Large Hadron Collider (LHC) at CERN including optics corrections and detecting faulty beam position monitors [40–42], for reconstruction of a storage ring’s linear optics based on Bayesian inference [43], to analyze beam position monitor placement in accelerators to find arrangements with the lowest probable predictive errors based on Bayesian Gaussian regression [44], surrogate models that map accelerator parameters to beam properties [45, 46], for temporal shaping of electron bunches in particle accelerators [47], for stabilization of source properties in synchrotron light sources [48], ML has been implemented with differentiable programming for physics applications [49], autoencoders have been developed to model accelerator sections [50], and ML has been used to represent many-body interactions with restricted-Boltzmann-machine neural networks [51].

## 1.2 Non-stationary Distributions

One of the main challenges faced by deep learning methods is large non-stationary systems whose characteristics change quickly with time for which re-training is not feasible. ML for non-stationary systems is an active field of research with recent results including the use of recurrent neural networks for speech perception in non-stationary noise [52], a method based on convolutional and recurrent neural networks has been proposed for modeling time-varying audio processors [53], complex-valued neural networks have been proposed for ML on non-stationary physical data and have shown that including phase information in feature maps improves both training and inference from deterministic physical data [54, 55], and methods have been developed for non-stationary systems which detect significant changes after which the weights of neural networks are updated/re-trained with new information or are continuously trained to keep up with continuous changes [56–58].

## 1.3 Overview of Main Results

We present a method for adaptive machine learning (AML) which does not require re-training. Our approach is based on adaptive tuning of the low-dimensional latent space of deep encoder-decoder style CNNs based on real-time feedback to quickly compensate for unknown and fast distribution shifts. We demonstrate our approach for predicting the properties of a time-varying charged particle beam in a particle accelerator whose components (accelerating electric fields and focusing magnetic fields) are also quickly changing with time. A schematic of the AML approach is shown in Figure 1. By squeezing our large input space (2709 dimensions in the particular example studied in this paper) down to a general nonlinear representation in a much lower dimensional latent space (100 in this case), we can quickly adaptively tune our system by utilizing the encoder-decoder representation learned by the CNN. This flexibility allows us to quickly respond to unknown disturbances and

changes, such as unknown changes of the input images and the input parameters, which create a difference between a function of the CNN's generated predictions and some related measurement. This general approach can be applied to a wide range of neural network structures, including 3D CNNs, and any adaptive feedback algorithm can be used for the adaptive feedback branch of the setup shown in Figure 1 such as stochastic gradient descent or robust conjugate search. In our case we prefer to use a recently developed robust extremum seeking (ES) feedback control algorithm which was originally designed for the stabilization of unknown open-loop unstable time-varying nonlinear systems and then extended for the optimization of many parameter time-varying unknown systems with noise-corrupted measurement functions [59, 60]. We have chosen this method because it can quickly tune many coupled parameters and has been applied for time-varying problems such as adaptively learning optimal feedback control policies for time-varying systems with unknown dynamics directly from measurement data [61].

## 2 Latent Space Tuning

### 2.1 Machine Learning, Dynamic Systems, and Control

Our approach of combining external feedback with neural networks is analogous to a natural phenomenon in biological systems in which networks of neurons interact with each other and are controlled by external feedback loops and other networks for tasks such as synchronization in the presence of delays, noise, and disturbances [62–66]. Some initial simplified adaptive ML studies have also begun on coupling the outputs of CNNs to adaptive feedback for real-time accelerator phase space control [67] and for predicting 3D electron density distributions for 3D coherent diffraction imaging [68]. Furthermore, powerful ML methods have recently been developed for control applications, for describing dynamic systems using advanced methods such as Koopman theory and dynamic mode decomposition, and for learning the partial differential equations that govern complex physical systems directly from data [69–74].

### 2.2 Adaptive Latent Space Tuning

Although in principal the results presented here are applicable to any type of neural network, we focus on convolutional encoder-decoder architectures as they have the most potential to benefit from this approach due to the incredibly large size of parameters within such networks which makes it difficult to re-train them quickly with small amounts of data. The inputs to our ML structure are a vector of scalar parameters of length  $N_p$ , an  $N \times N \times N_c$  image where  $N_c$  is the number of channels which for simplicity we will assume to be 1, and a vector of adaptively tuned control parameters of length  $N_L$ . Therefore our input feature space has total dimension  $N_{i,p} = N_L + N_p + N^2$  with  $N_l$  chosen as  $N_L \ll N_{i,p}$  with the network also designed to pinch down to a minimal latent space dimension of  $N_L$ .

When a  $N \times N$  input image represented by matrix

$$I^0 = \{I^0(i_0, j_0), i_0, j_0 \in \{1, 2, \dots, N\}\}, \quad (1)$$

passes through a stride 2 convolutional layer with a  $3 \times 3$  filter  $F_{0,ij}$  the output image size is reduced by a factor of 4 resulting in a  $N/2 \times N/2$  image  $I^1$  whose pixels are defined as

$$I_{i_1, j_1}^1 = f \left( b^0 + \sum_{i=-1}^1 \sum_{j=-1}^1 F_{0,ij} \times I_{i_0+i, j_0+j}^0 \right), \quad (2)$$

$$i_0, j_0 \in \{1, 3, \dots, \hat{N}\}, \quad i_1, j_1 \in \{1, 2, \dots, N/2\}, \quad (3)$$

where  $b^0$  is the bias and  $f$  a nonlinear activation function,  $\hat{N}$  is equal to  $N - 1$  if  $N$  is even and  $N$  if  $N$  is odd, with extra zeros padded onto the image for convolution with the filter in the case of odd  $N$ . Typically a collection of  $N_f > 1$  filters is used, which even for a single layer CNN would result in an output image of the form

$$I_{i_1, j_1}^1 = b^1 + \sum_{n=1}^{N_f} w_n \times f_n \left( b_n^0 + \sum_{i=-1}^1 \sum_{j=-1}^1 F_{0,ij,n} \times I_{i_0+i, j_0+j}^0 \right), \quad (4)$$

with  $11 \times N_f + 1$  total adjustable weights and biases for just a single layer CNN. For a wide encoder-decoder CNN with several layers the total number of adjustable parameters easily grows to hundreds of thousands very quickly and re-training requires large collections of new data sets. In our approach, as is typically the case with encoder-decoder CNNs, after several layers of convolutions we significantly reduce the size of a relatively large image ( $52 \times 52 \rightarrow 7 \times 7$ ) but use more and more filters at each stage, ending up with a tensor of shape  $N_i \times N_i \times N_f$  where  $N_i \times N_i$  is the final image size and  $N_f$  is the number of filters in the last convolution layer of the encoder. We then flatten the image into a vector and apply dense fully connected layers until we reach a low-dimensional latent space representation, a vector  $\mathbf{v}_L$  of length  $N_L \ll N_{i,p}$ , which we add to the  $N_L$  dimensional control input, a vector  $\mathbf{v}_c$  so that the latent space parameters are given by

$$\mathbf{p}_L = (p_1, \dots, p_{N_L}) = (v_1 + v_{c,1}, \dots, v_{N_L} + v_{c,N_L}) = \mathbf{v}_L + \mathbf{v}_{L,c}, \quad (5)$$

where the vector  $\mathbf{v}_L$  is automatically generated by the trained encoder portion of the network and the vector  $\mathbf{v}_{L,c}$  are controlled parameters that will be used for adaptive tuning later on, which are set to zero and have no influence during training. They will be used after training as inputs with which adaptive tuning of the latent space is possible. The vector  $\mathbf{p}_L$  is passed through additional fully connected dense layers before being reshaped into a small image ( $\sim 8 \times 8$ ) which then passes through a series of 2D transpose convolution layers until a collection of  $N_o$  output images of size  $N_{im} \times N_{im}$  are generated in a final layer with  $N_c$  channels with size  $\hat{I}(i, j, d) = N_{im} \times N_{im} \times N_c$ . Once the network is trained this collection of output images is a general nonlinear function (the generative branch of the network) of the parameters  $\mathbf{p}_L$  of the form

$$\hat{I}(i, j, d) = \mathbf{F}(\mathbf{p}_L, \mathbf{w}, \mathbf{b}, \{A\}), \quad i, j \in \{1, 2, \dots, N_o\}, \quad d \in \{1, 2, \dots, N_c\}, \quad (6)$$

where  $\mathbf{w}$  and  $\mathbf{b}$  are the weights and biases and  $\{A\}$  are the set of activation functions of the generative layers. Our prediction  $\hat{I}$  is our estimate of some unknown physical quantity  $I$  which we assume we cannot easily directly measure fully. In order to enable the adaptive feedback part of this procedure we must assume that we have some form of non-invasive online measurement of  $M(I(t))$  that can be compared to a simulated measurement of our prediction  $\hat{M}(\hat{I})$ , which we know how to approximate. For example we may be interested in a 6D density distribution but we only have direct measurements of one 2D projection. A detailed example and simulation study of such a problem for particle accelerator applications is presented in Section 3 below. Given our measurement and our simulated measurement of our prediction we then set up a dynamic feedback loop for minimization of a cost function of the form

$$C(\mathbf{p}_L(t), M(I(t))) = \mu \left( M(I(t)), \hat{M}(\hat{I}(\mathbf{p}_L(t))) \right), \quad (7)$$

$$\frac{\partial p_i}{\partial t} = \frac{\partial v_{c,i}}{\partial t} = \sqrt{\alpha \omega_i} \cos(\omega_i t + k C(\mathbf{p}_L(t), M(I(t)))), \quad (8)$$

where  $\mu$  is any metric that we define to quantify error, which may be something like the mean squared error between two 2D images:

$$\mu \left( M(i, j), \hat{M}(i, j) \right) = \frac{1}{N_x N_y} \sum_{i=1}^{N_x} \sum_{j=1}^{N_y} \left( M(i, j) - \hat{M}(i, j) \right)^2. \quad (9)$$

The adaptive feedback dynamics (8) are chosen based on the results in [59–61]. The hyper-parameters in (8) can intuitively be understood as  $\alpha$  representing a dithering amplitude which controls the size of the dynamic perturbations,  $k$  is a feedback gain, and the product  $k\alpha$  controls the speed of convergence and can be thought of as an overall learning rate. Finally the dithering frequencies  $\omega_i$  are chosen relative to a base frequency  $\omega$  such that they are distinct, of the form  $\omega_i = r_i \omega \neq r_j \omega = \omega_j$  for  $i \neq j$  such that no two frequencies are integer multiple of each other (such as distinct  $r_i \in [1, 1.75]$ ) because non-linearity typically introduce harmonics into the system dynamics. The convergence results for this feedback algorithm depend on the parameters being orthogonal in Hilbert space such that for any  $t > 0$  the  $L^2[0, t]$  inner product of two dithering functions is zero in the limit of large frequency  $\omega$ :

$$\lim_{\omega \rightarrow \infty} \int_0^t \cos(\omega_i \tau) \cos(\omega_j \tau) d\tau = 0. \quad (10)$$

In fact any orthogonal functions can be used, including non-differentiable and discontinuous square waves, as described in more detail in [59–61].

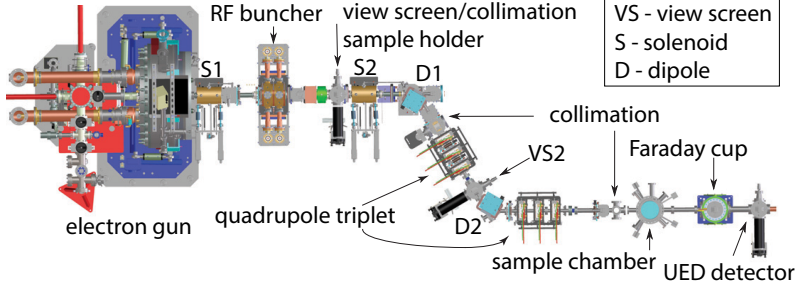


Figure 2: The HiRES ultrafast electron diffraction beamline is shown (adapted from [75]). For our work we care about the fact that the input beam distribution at the electron gun varies with time and the characteristics of the accelerator itself are also not perfectly reproducible including the magnetic fields of the solenoids and quadrupole magnets.

### 3 Particle Accelerator Application

Charged particle bunches in particle accelerators can be composed out of anywhere from  $10^5$  to  $10^{10}$  particles depending on the total charge. The charged particle dynamics are defined over a 6D phase space with density  $\rho(x, y, z, p_x, p_y, p_z)$  where  $(x, y, z)$  are the physical particle locations with  $z$  typically being the axis of acceleration and  $(x, y)$  the transverse off-axis distance. The components  $(p_x, p_y, p_z)$  are the components of particle momentum. All 6 dimensions are coupled through collective effects such as space charge forces which can simply be described as the electric fields of all of the individual particles pushing each other apart and via coherent synchrotron radiation in which accelerating charged particles release light which impacts other particles in the bunch thereby changing their energy [76]. The influence of collective effects grow as accelerators generate shorter more intense bunches such as 30 fs bunches at the SwissFEL X-ray FEL [77], sub 100 fs bunches for ultra fast electron diffraction (UED) [78], and picosecond bunch trains for UEDs and multicolor XFELs [79]. Our work focuses on the High Repetition-rate Electron Scattering apparatus (HiRES, shown in Fig. 2) at Lawrence Berkeley National Laboratory (LBNL), which accelerates pC-class, sub-picosecond long electron bunches up to one million times a second (MHz), providing some of the most dense 6D phase space among accelerators at unique repetition rates, making it an ideal test bed for advanced algorithm development [75, 80].

In order to better understand and compensate for collective effects in intense beams it would be very helpful to have a view of the full 6D phase space in real time, which is of course impossible. What is usually possible is to record various 2D projections of a beam's 6D phase space. For example, it is possible to measure the longitudinal phase space (LPS) of a charged particle bunch by using a transverse deflecting radio frequency resonant cavity (TCAV) which measures  $(z, p_z)$  or equivalently  $(z, E)$  where  $E$  is the relativistic kinetic energy related to the relativistic momentum  $p_z$ .

Although physics and machine learning-based surrogate models can potentially serve as non-invasive beam diagnostics, the main challenges they face are uncertainty in and time-variation of accelerator components, such as magnets and accelerating resonant cavities, and the time-variation of the initial beam distribution entering the accelerator. Such distributions drift with time requiring lengthy measurements that interrupt accelerator operations. One approach to adaptively tune an online physics model has been developed which attempted to track time-varying electron beam properties at the Facility for Advanced Accelerator Experimental Tests (FACET) at SLAC National Accelerator Laboratory by comparing the model's predictions to a non-invasive energy spread spectrum measurement [81]. Although the adaptive model tuning approach at FACET was able to track the beam's LPS its main limitations were the relatively slow speed of the physics model (several seconds for one simulation) and also that its accuracy was limited by the fact that there was no access to a good estimate of the time varying input beam distribution to set the initial conditions in the model.

Therefore we propose to utilize AML to develop a virtual diagnostic that is able to provide information about the beam's phase space by using only available 2D measurements of the LPS  $(z, E)$ . The first goal is to develop a model which captures all of the relationships and correlations between the various phase space slices for a particular accelerator. Because the 6D phase space dynamics are coupled and the charged particles evolve under physics constraints unique to a given accelerator lattice, it

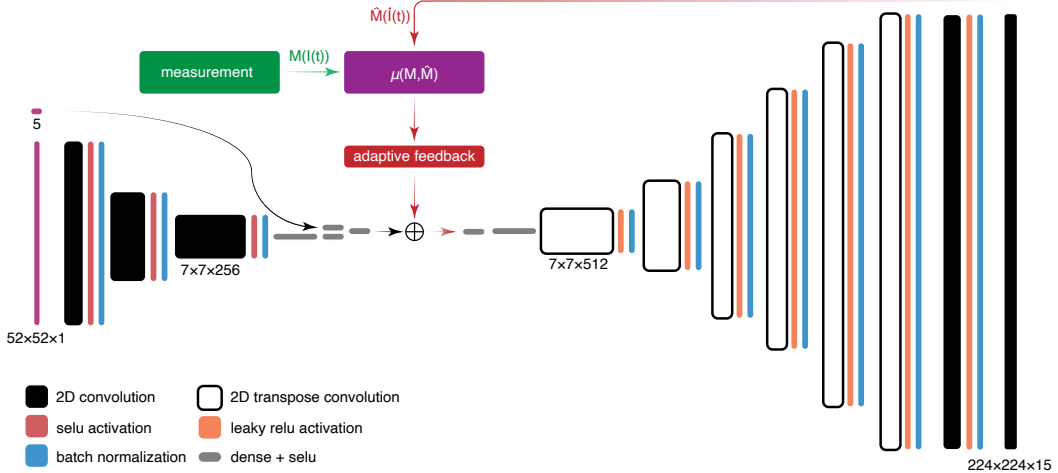


Figure 3: A detailed view of the CNN structure for the AML setup is shown.

may be possible to uniquely recover or track various 2D slices of the 6D phase space based on just a single 2D measurement. In general (collision-less approximation) the 6D phase space distribution  $\rho(x, y, z, p_x, p_y, p_z)$  satisfies the relativistic Vlasov equation

$$\frac{\partial \rho}{\partial t} + \mathbf{v} \cdot \nabla_{\mathbf{x}} \rho + \dot{\mathbf{p}} \cdot \nabla_{\mathbf{p}} \rho = 0, \quad \mathbf{v} = (\dot{x}, \dot{y}, \dot{z}), \quad \mathbf{p} = (p_x, p_y, p_z) \quad (11)$$

$$\dot{\mathbf{p}} = q(\mathbf{E} + \mathbf{v} \times \mathbf{B}), \quad \mathbf{p} = \gamma m \mathbf{v}, \quad \gamma = \frac{1}{\sqrt{1 - \frac{v^2}{c^2}}}, \quad v = |\mathbf{v}|, \quad (12)$$

where the electric and magnetic fields include all of the contributions from the charges within the bunch as well as all of the external electromagnetic fields introduced by components of the accelerator such as radio frequency (RF) resonant accelerating cavities, solenoids, dipoles, and quadrupole magnets. To learn the correlations within the HiRES electron beam we simulated the evolution of approximately 210 thousand sets of various initial beam distributions and accelerator parameter settings  $\mathbf{p} = (p_1, \dots, p_5)$  which were the beam energy at the accelerator entrance, the phase of the RF electromagnetic field in the gun generating the beam, the peak field in the buncher cavity directly after the gun, the buncher RF field phase, and the solenoid magnet's current. For each simulation we would record the randomized initial  $52 \times 52$  pixel  $(x, y)$  beam distribution and all 15 2D slice combinations of the final 6D beam distribution down stream which were recorded as 15 images of size  $224 \times 224$  pixels. An encoder-decoder type CNN was then trained which took the initial  $(x, y)$  beam distribution as well as the accelerator parameters  $\mathbf{p}$  as inputs. Once the network was trained, we tested if we could recover the  $\rho_{x, x'}(x, x')$  and  $\rho_{y, y'}(y, y')$  transverse 2D phase space distributions by adaptively matching the network's prediction of the 2D longitudinal phase space distribution  $\rho_{z, E}(z, E)$ , with the 2D distributions being the 2D projections for the 6D phase space:

$$\rho_{x, x'}(x, x') = \int_y \int_{y'} \int_z \int_E \rho(x, y, z, x', y', E) dy dy' dz dE, \quad (13)$$

$$\rho_{y, y'}(y, y') = \int_x \int_{x'} \int_z \int_E \rho(x, y, z, x', y', E) dx dx' dz dE, \quad (14)$$

$$\rho_{z, E}(z, E) = \int_x \int_{x'} \int_y \int_{y'} \rho(x, y, z, x', y', E) dx dx' dy dy', \quad (15)$$

where  $x' = p_x/p_z$  and  $y' = p_y/p_z$  are angles at which electrons fly relative to the accelerator's axis. The setup is shown in Figure 4.

To demonstrate the effectiveness of the scheme we chose an input beam distribution and input parameter values that were outside of the range of values used to train the network and the associated output beam phase space slices. Then, as input to the network we simply used the mean input image and input parameter values computer over all of the training data, because in a real world application

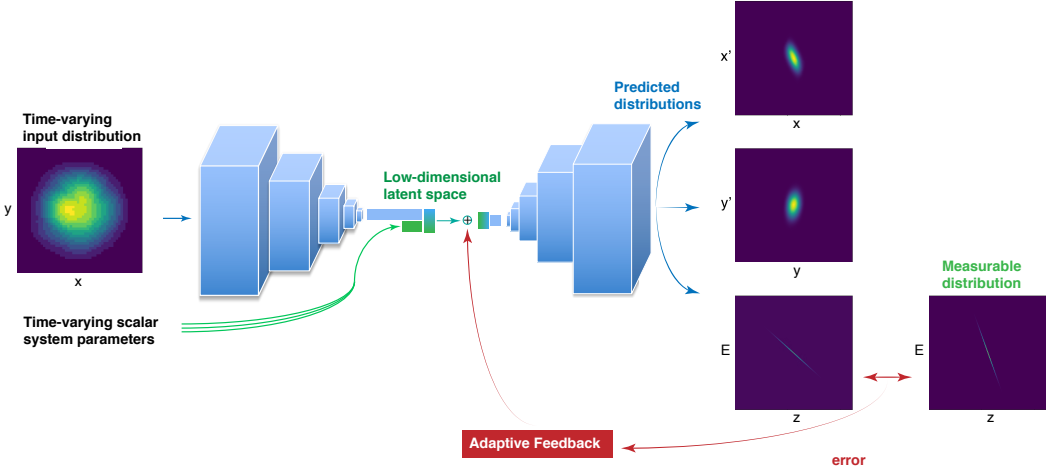


Figure 4: Adaptive latent space tuning setup for predicting the transverse phase space of the HiRES beam based only on longitudinal phase space measurements.

we would not have access (unless we interrupt operations and perform lengthy dedicated procedures to find it) to a measurement of the time-varying input beam distribution and we would only know rough estimates of the 5 input parameters described above. We then used the adaptive feedback based purely on a comparison of the predicted and measurable  $(z, E)$  phase space slices based on the mean squared error (MSE) as defined in Equation (9) which we minimized by iteratively tuning 100 parameters  $\mathbf{v}_{L,c} = (v_{c,1}, \dots, v_{c,100})$  that are added at the low dimensional latent space middle of the CNN, in order to match the measured  $(z, E)$  phase space in order to recover estimates of the transverse phase space  $(x, x')$ ,  $(y, y')$ . During this tuning we also kept track of MSE between the transverse phase spaces and their predictions. Results of adaptively tuning the latent space based only on comparisons of the  $(z, E)$  2D phase space projections are shown in Figures 5 and 6. In both cases we use input beam distributions and parameter settings outside of the range of the training data. The distribution and accelerator parameters used in Figure 5 were closer to the training set and resulted in a very close match between all 3 phase space projections. For a distribution and parameter settings further away from the training set, as expected the matches were worse, but still impressive as shown in Figure 5. A degradation in predictive power as we move further and further from the span of the training set is expected because even with the learned relationships between the phase space projections and even with the constraints provided by the beam dynamics and the particular components of HiRES, there is still no guarantee that a match of the  $(z, E)$  distributions will result in a unique reconstruction of the associated transverse phase space.

## 4 Conclusions

We have demonstrated a new approach to machine learning for time-varying systems by adaptively tuning the nonlinear low dimensional latent space representation of complex systems. The dimensionality reduction in this case took an input image of dimensions  $52 \times 52 = 2704$  plus 5 input parameters down to a 100 dimensional latent space representation which is only  $\sim 3\%$  of the original, which allows us to tune in real-time. Furthermore, we have demonstrated an approach that has taught the encoder-decoder the relationships between the various 2D projections of a 6D phase space for the HiRES compact accelerator, which allows us to predict and track the transverse phase space based only on longitudinal phase space measurements. We believe that this approach can be used for a wide range of machine learning problems in which there is limited data available for making predictions after a network has been trained to learn underlying relationships and also for problems with time-varying non-stationary distributions, for which this approach has the potential to produce the correct predictions in an iterative fashion as was demonstrated here by predicting unseen beam distributions. Such an approach can be extremely useful for all advanced particle accelerators with online real-time  $(z, E)$  longitudinal phase space diagnostics such as FACET-II, LCLS, LCLS-II, EuXFEL, and SwissFEL.

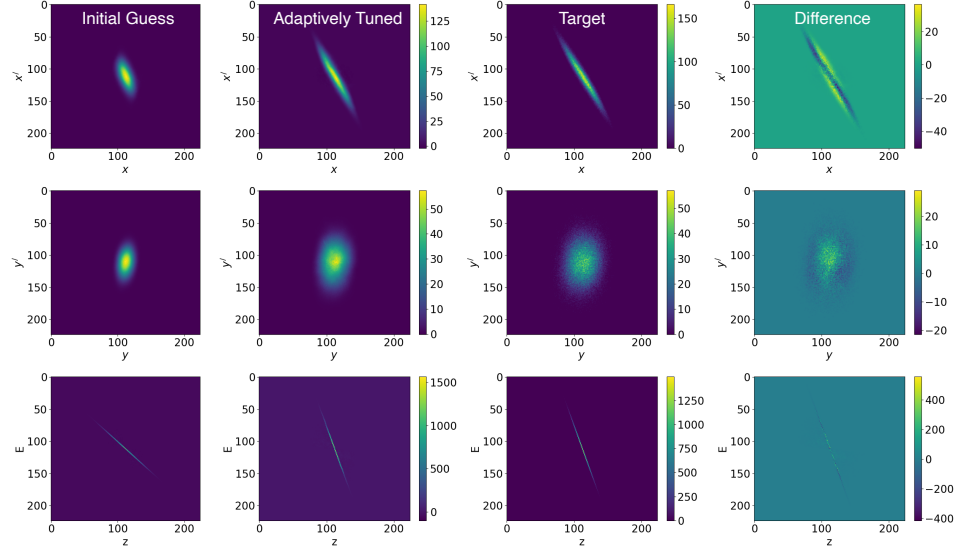


Figure 5: Results of adaptively tuning the latent space based only on comparisons of the  $(z, E)$  2D phase space projections which resulted in a very close match of all 3 phase space projections.

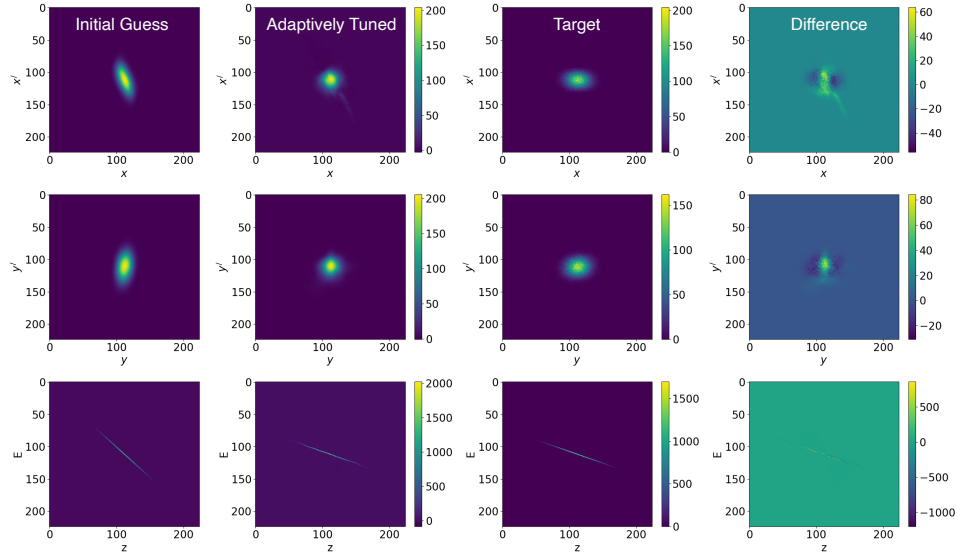


Figure 6: Results of adaptively tuning the latent space based only on comparisons of the  $(z, E)$  2D phase space projections which resulted in a close estimate, but a slightly less accurate match of the transverse phase space projections. This is expected, as unseen distributions are tested that are further and further from the training set we do expect this method to break down since a match of the  $(z, E)$  distributions does not guarantee a unique reconstruction of the associated transverse phase space.

## References

- [1] Trevor Hastie, Robert Tibshirani, and Jerome Friedman. *The elements of statistical learning: data mining, inference, and prediction*. Springer Science & Business Media, 2009.
- [2] Kevin P Murphy. *Machine learning: a probabilistic perspective*. MIT press, 2012.
- [3] Yann LeCun, Yoshua Bengio, and Geoffrey Hinton. Deep learning. *nature*, 521(7553):436–444, 2015.
- [4] Michael I Jordan and Tom M Mitchell. Machine learning: Trends, perspectives, and prospects. *Science*, 349(6245):255–260, 2015.
- [5] Alex Krizhevsky, Ilya Sutskever, and Geoffrey E Hinton. Imagenet classification with deep convolutional neural networks. *Advances in neural information processing systems*, 25:1097–1105, 2012.
- [6] Max Jaderberg, Karen Simonyan, Andrew Zisserman, and Koray Kavukcuoglu. Spatial transformer networks. *arXiv preprint arXiv:1506.02025*, 2015.
- [7] Jonas Pfeiffer, Andreas Rücklé, Clifton Poth, Aishwarya Kamath, Ivan Vulić, Sebastian Ruder, Kyunghyun Cho, and Iryna Gurevych. Adapterhub: A framework for adapting transformers. *arXiv preprint arXiv:2007.07779*, 2020.
- [8] Hugo Touvron, Matthieu Cord, Alexandre Sablayrolles, Gabriel Synnaeve, and Hervé Jégou. Going deeper with image transformers. *arXiv preprint arXiv:2103.17239*, 2021.
- [9] Yoshua Bengio, Patrice Simard, and Paolo Frasconi. Learning long-term dependencies with gradient descent is difficult. *IEEE transactions on neural networks*, 5(2):157–166, 1994.
- [10] Sepp Hochreiter and Jürgen Schmidhuber. Long short-term memory. *Neural computation*, 9(8):1735–1780, 1997.
- [11] Jaehoon Lee, Yasaman Bahri, Roman Novak, Samuel S Schoenholz, Jeffrey Pennington, and Jascha Sohl-Dickstein. Deep neural networks as gaussian processes. *arXiv preprint arXiv:1711.00165*, 2017.
- [12] Lechao Xiao, Jeffrey Pennington, and Samuel Schoenholz. Disentangling trainability and generalization in deep neural networks. In *International Conference on Machine Learning*, pages 10462–10472. PMLR, 2020.
- [13] Volodymyr Mnih, Koray Kavukcuoglu, David Silver, Andrei A Rusu, Joel Veness, Marc G Bellemare, Alex Graves, Martin Riedmiller, Andreas K Fidjeland, Georg Ostrovski, et al. Human-level control through deep reinforcement learning. *nature*, 518(7540):529–533, 2015.
- [14] Richard S Sutton and Andrew G Barto. *Reinforcement learning: An introduction*. MIT press, 2018.
- [15] Martín Abadi, Paul Barham, Jianmin Chen, Zhifeng Chen, Andy Davis, Jeffrey Dean, Matthieu Devin, Sanjay Ghemawat, Geoffrey Irving, Michael Isard, et al. Tensorflow: A system for large-scale machine learning. In *12th {USENIX} symposium on operating systems design and implementation ({OSDI} 16)*, pages 265–283, 2016.
- [16] Martín Abadi, Ashish Agarwal, Paul Barham, Eugene Brevdo, Zhifeng Chen, Craig Citro, Greg S Corrado, Andy Davis, Jeffrey Dean, Matthieu Devin, et al. Tensorflow: Large-scale machine learning on heterogeneous distributed systems. *arXiv preprint arXiv:1603.04467*, 2016.
- [17] Yangqing Jia, Evan Shelhamer, Jeff Donahue, Sergey Karayev, Jonathan Long, Ross Girshick, Sergio Guadarrama, and Trevor Darrell. Caffe: Convolutional architecture for fast feature embedding. In *Proceedings of the 22nd ACM international conference on Multimedia*, pages 675–678, 2014.
- [18] Frank Seide and Amit Agarwal. Cntk: Microsoft’s open-source deep-learning toolkit. In *Proceedings of the 22nd ACM SIGKDD International Conference on Knowledge Discovery and Data Mining*, pages 2135–2135, 2016.
- [19] The Theano Development Team, Rami Al-Rfou, Guillaume Alain, Amjad Almahairi, Christof Angermueller, Dzmitry Bahdanau, Nicolas Ballas, Frédéric Bastien, Justin Bayer, Anatoly Belikov, et al. Theano: A python framework for fast computation of mathematical expressions. *arXiv preprint arXiv:1605.02688*, 2016.
- [20] Adam Paszke, Sam Gross, Francisco Massa, Adam Lerer, James Bradbury, Gregory Chanan, Trevor Killeen, Zeming Lin, Natalia Gimelshein, Luca Antiga, et al. Pytorch: An imperative style, high-performance deep learning library. *arXiv preprint arXiv:1912.01703*, 2019.
- [21] Keith T Butler, Daniel W Davies, Hugh Cartwright, Olexandr Isayev, and Aron Walsh. Machine learning for molecular and materials science. *Nature*, 559(7715):547–555, 2018.
- [22] Darko Zibar, Henk Wymeersch, and Ilya Lyubomirsky. Machine learning under the spotlight. *Nature Photonics*, 11(12):749–751, 2017.
- [23] Ekin D Cubuk, Samuel Stern Schoenholz, Jennifer M Rieser, Brad Dean Malone, Joerg Rottler, Douglas J Durian, Eftimios Kaxiras, and Andrea J Liu. Identifying structural flow defects in disordered solids using machine-learning methods. *Physical review letters*, 114(10):108001, 2015.

[24] Samuel S Schoenholz, Ekin D Cubuk, Daniel M Sussman, Efthimios Kaxiras, and Andrea J Liu. A structural approach to relaxation in glassy liquids. *Nature Physics*, 12(5):469–471, 2016.

[25] Samuel S Schoenholz. Combining machine learning and physics to understand glassy systems. In *Journal of Physics: Conference Series*, volume 1036, page 012021. IOP Publishing, 2018.

[26] Maitane Berecibar. Machine-learning techniques used to accurately predict battery life, 2019.

[27] Shaozhi Li, Philip M Dee, Ehsan Khatami, and Steven Johnston. Accelerating lattice quantum monte carlo simulations using artificial neural networks: Application to the holstein model. *Physical Review B*, 100(2): 020302, 2019. doi: <https://doi.org/10.1103/PhysRevB.100.020302>.

[28] Alessandro Muscoloni, Josephine Maria Thomas, Sara Ciucci, Ginestra Bianconi, and Carlo Vittorio Cannistraci. Machine learning meets complex networks via coalescent embedding in the hyperbolic space. *Nature communications*, 8(1):1–19, 2017.

[29] Joshua L Lansford and Dionisios G Vlachos. Infrared spectroscopy data-and physics-driven machine learning for characterizing surface microstructure of complex materials. *Nature communications*, 11(1): 1–12, 2020.

[30] Alexandre Tkatchenko. Machine learning for chemical discovery. *Nature Communications*, 11(1):1–4, 2020.

[31] Frank Cichos, Kristian Gustavsson, Bernhard Mehlig, and Giovanni Volpe. Machine learning for active matter. *Nature Machine Intelligence*, 2(2):94–103, 2020.

[32] Alexander Radovic, Mike Williams, David Rousseau, Michael Kagan, Daniele Bonacorsi, Alexander Himmel, Adam Aurisano, Kazuhiro Terao, and Taritree Wongjirad. Machine learning at the energy and intensity frontiers of particle physics. *Nature*, 560(7716):41–48, 2018.

[33] Rino Ragno, Rosanna Papa, Alexandros Patsilinakos, Gianluca Vrenna, Stefania Garzoli, Vanessa Tuccio, Ersilia Vita Fiscarelli, Laura Selan, and Marco Artini. Essential oils against bacterial isolates from cystic fibrosis patients by means of antimicrobial and unsupervised machine learning approaches. *Scientific reports*, 10(1):1–11, 2020.

[34] Dmitry S Bulgarevich, Susumu Tsukamoto, Tadashi Kasuya, Masahiko Demura, and Makoto Watanabe. Pattern recognition with machine learning on optical microscopy images of typical metallurgical microstructures. *Scientific reports*, 8(1):1–8, 2018.

[35] Ghanshyam Pilania, Arun Mannodi-Kanakkithodi, BP Uberuaga, Rampi Ramprasad, JE Gubernatis, and Turab Lookman. Machine learning bandgaps of double perovskites. *Scientific reports*, 6(1):1–10, 2016.

[36] Yu-Feng Shen, Reeju Pokharel, Thomas J Nizolek, Anil Kumar, and Turab Lookman. Convolutional neural network-based method for real-time orientation indexing of measured electron backscatter diffraction patterns. *Acta Materialia*, 170:118–131, 2019.

[37] Auralee Edelen, Nicole Neveu, Matthias Frey, Yannick Huber, Christopher Mayes, and Andreas Adelmann. Machine learning for orders of magnitude speedup in multiobjective optimization of particle accelerator systems. *Physical Review Accelerators and Beams*, 23(4):044601, 2020.

[38] Joseph Duris, Dylan Kennedy, Adi Hanuka, Jane Shtalenkova, Auralee Edelen, P Baxevanis, Adam Egger, T Cope, M McIntire, S Ermon, et al. Bayesian optimization of a free-electron laser. *Physical review letters*, 124(12):124801, 2020.

[39] X Ren, A Edelen, A Lutman, G Marcus, T Maxwell, and D Ratner. Temporal power reconstruction for an x-ray free-electron laser using convolutional neural networks. *Physical Review Accelerators and Beams*, 23(4):040701, 2020.

[40] Elena Fol, JM Coello de Portugal, Giuliano Franchetti, and Rogelio Tomás. Optics corrections using machine learning in the lhc. In *Proceedings of the 2019 International Particle Accelerator Conference, Melbourne, Australia*, 2019.

[41] Elena Fol, JM Coello de Portugal, Rogelio Tomás, et al. Unsupervised machine learning for detection of faulty beam position monitors. In *Proc. 10th Int. Particle Accelerator Conf.(IPAC'19), Melbourne, Australia*, volume 2668, 2019.

[42] Pasquale Arpaia, Gabriella Azzopardi, Frederic Blanc, Giuseppe Bregliozi, Xavier Buffat, Loic Coyle, Elena Fol, Francesco Giordano, Massimo Giovannozzi, Tatiana Pieloni, et al. Machine learning for beam dynamics studies at the cern large hadron collider. *Nuclear Instruments and Methods in Physics Research Section A: Accelerators, Spectrometers, Detectors and Associated Equipment*, 985:164652, 2021.

[43] Yue Hao, Yongjun Li, Michael Balcewicz, Leo Neufcourt, and Weixing Cheng. Reconstruction of storage ring's linear optics with bayesian inference. *arXiv preprint arXiv:1902.11157*, 2019.

[44] Yongjun Li, Yue Hao, Weixing Cheng, and Robert Rainer. Analysis of beam position monitor requirements with bayesian gaussian regression. *arXiv preprint arXiv:1904.05683*, 2019.

[45] C Emma, A Edelen, MJ Hogan, B O’Shea, G White, and V Yakimenko. Machine learning-based longitudinal phase space prediction of particle accelerators. *Physical Review Accelerators and Beams*, 21(11):112802, 2018.

[46] Adi Hanuka, Claudio Emma, Timothy Maxwell, Alan S Fisher, Bryce Jacobson, MJ Hogan, and Zhirong Huang. Accurate and confident prediction of electron beam longitudinal properties using spectral virtual diagnostics. *Scientific Reports*, 11(1):1–10, 2021.

[47] Jinyu Wan, Yi Jiao, and Juhao Wu. Machine learning-based direct solver for one-to-many problems of temporal shaping of electron bunches. *arXiv preprint arXiv:2103.06594*, 2021.

[48] SC Leemann, S Liu, A Hexemer, MA Marcus, CN Melton, H Nishimura, and C Sun. Demonstration of machine learning-based model-independent stabilization of source properties in synchrotron light sources. *Physical review letters*, 123(19):194801, 2019.

[49] Samuel Schoenholz and Ekin Dogus Cubuk. Jax md: a framework for differentiable physics. *Advances in Neural Information Processing Systems*, 33, 2020.

[50] Jun Zhu, Ye Chen, Frank Brinker, Winfried Decking, Sergey Tomin, and Holger Schlarb. Deep learning-based autoencoder for data-driven modeling of an rf photoinjector. *arXiv preprint arXiv:2101.10437*, 2021.

[51] Ermal Rrapaj and Alessandro Roggero. Exact representations of many-body interactions with restricted-boltzmann-machine neural networks. *Physical Review E*, 103(1):013302, 2021. doi: <https://doi.org/10.1103/PhysRevE.103.013302>.

[52] Tobias Goehring, Mahmoud Keshavarzi, Robert P Carlyon, and Brian CJ Moore. Using recurrent neural networks to improve the perception of speech in non-stationary noise by people with cochlear implants. *The Journal of the Acoustical Society of America*, 146(1):705–718, 2019.

[53] Marco A Martínez Ramírez, Emmanouil Benetos, and Joshua D Reiss. A general-purpose deep learning approach to model time-varying audio effects. *arXiv preprint arXiv:1905.06148*, 2019.

[54] Golara Javadi, Minh Nguyen Nhat To, Samareh Samadi, Sharareh Bayat, Samira Sojoudi, Antonio Hurtado, Silvia Chang, Peter Black, Parvin Mousavi, and Purang Abolmaesumi. Complex cancer detector: Complex neural networks on non-stationary time series for guiding systematic prostate biopsy. In *International Conference on Medical Image Computing and Computer-Assisted Intervention*, pages 524–533. Springer, 2020.

[55] Jesper Sören Dramsch, Mikael Lüthje, and Anders Nymark Christensen. Complex-valued neural networks for machine learning on non-stationary physical data. *Computers & Geosciences*, 146:104643, 2021.

[56] Roberto Calandra, Tapani Raiko, Marc Peter Deisenroth, and Federico Montesino Pouzols. Learning deep belief networks from non-stationary streams. In *International Conference on Artificial Neural Networks*, pages 379–386. Springer, 2012.

[57] Arief Koesdwiady, Safaa Bedawi, Chaojie Ou, and Fakhri Karray. Non-stationary traffic flow prediction using deep learning. In *2018 IEEE 88th Vehicular Technology Conference (VTC-Fall)*, pages 1–5. IEEE, 2018.

[58] Richard Kurle, Botond Cseke, Alexej Klushyn, Patrick van der Smagt, and Stephan Günnemann. Continual learning with bayesian neural networks for non-stationary data. In *International Conference on Learning Representations*, 2019.

[59] Alexander Scheinker and Miroslav Krstić. Minimum-seeking for clfs: Universal semiglobally stabilizing feedback under unknown control directions. *IEEE Transactions on Automatic Control*, 58(5):1107–1122, 2012.

[60] Alexander Scheinker and David Scheinker. Bounded extremum seeking with discontinuous dithers. *Automatica*, 69:250–257, 2016.

[61] Alexander Scheinker and David Scheinker. Extremum seeking for optimal control problems with unknown time-varying systems and unknown objective functions. *International Journal of Adaptive Control and Signal Processing*, 2020.

[62] Hirotaka Doho, Sou Nobukawa, Haruhiko Nishimura, Nobuhiko Wagatsuma, and Tetsuya Takahashi. Transition of neural activity from the chaotic bipolar-disorder state to the periodic healthy state using external feedback signals. *Frontiers in Computational Neuroscience*, 14:76, 2020.

[63] Malik Muhammad Ibrahim and Il Hyo Jung. Complex synchronization of a ring-structured network of fitzhugh-nagumo neurons with single-and dual-state gap junctions under ionic gates and external electrical disturbance. *IEEE Access*, 7:57894–57906, 2019.

[64] Malik Muhammad Ibrahim, Muhammad Ahmad Kamran, Malik Muhammad Naeem Mannan, Il Hyo Jung, and Sangil Kim. Lag synchronization of coupled time-delayed fitzhugh–nagumo neural networks via feedback control. *Scientific reports*, 11(1):1–15, 2021.

[65] Sou Nobukawa, Natsusaku Shibata, Haruhiko Nishimura, Hirotaka Doho, Nobuhiko Wagatsuma, and Teruya Yamanishi. Resonance phenomena controlled by external feedback signals and additive noise in neural systems. *Scientific reports*, 9(1):1–15, 2019.

[66] Sou Nobukawa and Natsusaku Shibata. Controlling chaotic resonance using external feedback signals in neural systems. *Scientific reports*, 9(1):1–9, 2019.

[67] Alexander Scheinker, Auralee Edelen, Dorian Bohler, Claudio Emma, and Alberto Lutman. Demonstration of model-independent control of the longitudinal phase space of electron beams in the linac-coherent light source with femtosecond resolution. *Physical review letters*, 121(4):044801, 2018. doi: <https://doi.org/10.1103/PhysRevLett.121.044801>.

[68] Alexander Scheinker and Reetu Pokharel. Adaptive 3d convolutional neural network-based reconstruction method for 3d coherent diffraction imaging. *Journal of Applied Physics*, 128(18):184901, 2020.

[69] Jonathan H Tu, Clarence W Rowley, Dirk M Luchtenburg, Steven L Brunton, and J Nathan Kutz. On dynamic mode decomposition: Theory and applications. *arXiv preprint arXiv:1312.0041*, 2013.

[70] Steven L Brunton, Joshua L Proctor, and J Nathan Kutz. Discovering governing equations from data by sparse identification of nonlinear dynamical systems. *Proceedings of the national academy of sciences*, 113(15):3932–3937, 2016.

[71] Samuel H Rudy, Steven L Brunton, Joshua L Proctor, and J Nathan Kutz. Data-driven discovery of partial differential equations. *Science Advances*, 3(4):e1602614, 2017.

[72] Bethany Lusch, J Nathan Kutz, and Steven L Brunton. Deep learning for universal linear embeddings of nonlinear dynamics. *Nature communications*, 9(1):1–10, 2018.

[73] Steven L Brunton and J Nathan Kutz. *Data-driven science and engineering: Machine learning, dynamical systems, and control*. Cambridge University Press, 2019.

[74] Steven L Brunton, Bernd R Noack, and Petros Koumoutsakos. Machine learning for fluid mechanics. *Annual Review of Fluid Mechanics*, 52:477–508, 2020.

[75] D Filippetto and H Qian. Design of a high-flux instrument for ultrafast electron diffraction and microscopy. *Journal of Physics B: Atomic, Molecular and Optical Physics*, 49(10):104003, 2016. URL <https://iopscience.iop.org/article/10.1088/0953-4075/49/10/104003/meta>.

[76] Lev Davidovich Landau. *The classical theory of fields*, volume 2. Elsevier, 2013.

[77] Alexander Malyzhenkov, Yunieski P Arbelo, Paolo Craievich, Philipp Dijkstal, Eugenio Ferrari, Sven Reiche, Thomas Schietinger, Pavle Juranić, and Eduard Prat. Single-and two-color attosecond hard x-ray free-electron laser pulses with nonlinear compression. *Physical Review Research*, 2(4):042018, 2020. doi: <https://doi.org/10.1103/PhysRevResearch.2.042018>.

[78] T Van Oudheusden, PLEM Pasman, SB Van Der Geer, MJ De Loos, MJ Van Der Wiel, and OJ Luiten. Compression of subrelativistic space-charge-dominated electron bunches for single-shot femtosecond electron diffraction. *Physical review letters*, 105(26):264801, 2010. doi: <https://doi.org/10.1103/PhysRevLett.105.264801>.

[79] Francois Lemery, Philippe Piot, Gayane Amatuni, Prach Boonpornprasert, Y Chen, J Good, Bagrat Grigoryan, Matthias Gross, M Krasilnikov, Osip Lishilin, et al. Passive ballistic microbunching of nonultrarelativistic electron bunches using electromagnetic wakefields in dielectric-lined waveguides. *Physical review letters*, 122(4):044801, 2019. doi: <https://doi.org/10.1103/PhysRevLett.122.044801>.

[80] F Ji, Daniel B Durham, Andrew M Minor, Pietro Musumeci, Jorge G Navarro, and Daniele Filippetto. Ultrafast relativistic electron nanoprobes. *Communications Physics*, 2(1):1–10, 2019. doi: <https://doi.org/10.1038/s42005-019-0154>.

[81] Alexander Scheinker and Spencer Gessner. Adaptive method for electron bunch profile prediction. *Physical Review Special Topics-Accelerators and Beams*, 18(10):102801, 2015.